Dynamic Fluid-Structure Interaction Analysis of Propeller Aircraft Wing

Intizar Ali[a*], Abdul Hameed Memon[b], M. Tarique Bhatti[c], Dileep Kumar[d],

Ishfaque Ali Qazi[e], Sajjad Banghwar[f]

[a]*Deptt. of Mechanical Engineering, The Benazir Bhutto Shaheed University of technology and skill development Khairpur Mir's, Pakistan*

[b]*Deptt. of Mechanical Engineering, Hamdard University Karachi, Pakistan*

[c,f,e]*Deptt. of Mechanical Engineering, Quaid-e-Awam University College of Engineering Science and Technology, Larkana, Pakistan*

[d]*Deptt. of Mechanical Engineering, MUET, Shaheed Zulfiqar Ali Bhutto Campus, Khairpur Mir's, Pakistan*

[a]*Email: intizar_tunio@hotmail.com,* [b]*Email: hameed.memon@hamdard.edu.pk,* [c]*Email: trqbhatti@hotmail.com*

[d]*Email: dileepkumar@muetkhp.edu.pk,* [e]*Email: ishfaque@hotmail.com,* [f]*Email: sajjadbhangwar@gmail.com*

Abstract

During flight, aircraft wing is subjected to time dependent loads resulting in wing deformation and oscillation which is a challenge to its structural design as well as safety. At present, structural integrity and wing performance are mostly evaluated on the basis of static loading only. While dynamic loading has got minor attention due to this research work analyses structural and aerodynamic behavior of rectangular aircraft wing under time varying conditions. The effects of structural non-linearity were also taken into account. Computational Fluid Dynamics (CFD) and Computational Structural Dynamics (CSD) codes were coupled to predict aerodynamic performance of deformable wing structure. To analyze and compare the performance of rigid and flexible Aluminum alloy 7075 T6 wing were simulated. Research results reveal that there is 5.64% decrease in Lift-to-Drag ratio by considering wing as flexible structure. The analysis of wing structural behavior by varying fluid forces showed that wing behavior is highly non-linear in nature; therefore dynamic loading conditions are highly important to consider.

Keywords: Fluid-Structure Interaction; Propeller aircraft; Computational Fluid Dynamics; Computational Structural Dynamics.

----

* Corresponding author.

1. Introduction

In aircrafts, fluid-structure interaction is the direct interaction of deformable structure (such as wing, fuselage, tail etc.) with its surrounding fluid. Interaction between fluid and flexible structure have got extreme importance in many engineering applications, due to various undesired phenomena's such as fluttering, buffeting and collapsing of bridges and cooling towers, fluid-excited vibration of tall building and wind turbine blades, wind-plants interaction, as well as flutter in aircraft wings [1-8]. The number of researches was conducted to evaluate the need for FSI analysis in aircrafts components design. Their research comes with this conclusion that FSI analysis is highly important for the efficient and lightweight structure of various aircraft components especially wing, aileron as well as winglets [9, 10]. Research carried out aero elastic analysis of High Aspect Ratio (HAR) wing to analyze effect of wing deformation on aerodynamic characteristics. Showed that wing deformation causes decrease in flutter speed and aircraft safety [11]. Tielin, 2008 conducted research on (HAR) flexible wing to analyze aero elastic effects on its aerodynamic characteristic. His research revealed that lift/drag ratio is significantly affected by wing deformation [12] .Experimental studies was conducted on (HAR) sweep forward wing to analyze effect of wing bending and its twisting on aerodynamic efficiency. This research showed that wing deformation cause drop in lift/drag ratio [13]. Static aero-elastic analysis of aircraft wing was carried out to analyze effect of wing deformation on its aerodynamic efficiency. It was found that elastic wing experience bending and twisting due to that 27.9% decrease in lift force was observed [14]. FSI analysis of (HAR) composite wing of Unmanned Arial Vehicle (UAV) was conducted under cruise time predict behaviour of composite material. The study concluded that composite wing is light in weight and possesses good bending and torsional properties [15]. Another research conducted static aero-elastic analysis of composite wing at various flight speeds results showed that deformation increases with increase in aircraft speed and angle of attack [16]. Study conducted to predict effect of hovering hoverflies wing deformation on lift, drag and power coefficient by considering camber deformation along with span wise twist. significant difference in lift and power coefficient of wings was noticed [17]. Variable camber airfoil was analyzed to find effect on aerodynamic efficiency due to deformation under gust wind. The results indicated that camber deformation affects aerodynamic efficiency and with increase in deformation results increase in mean thrust and propulsive efficiency [18].From literature review it was concluded that lot of research was conducted on fluid- structure interaction analysis of aircraft wing by but almost all the previous researches related to static fluid structure interaction analysis. But aircraft is flying under diverse atmospheric conditions where it is subjected to unpredictable time-dependent aerodynamic loads. Due to aerodynamic loads wing deforms which is highly dangerous for aircraft safety as well as for stability and it may also affects aircraft performance. Therefore this research was conducted to analyze effect of wing deformation of on aerodynamic efficiency of aircraft.

2. Mathematical Modeling

The coupled dynamic fluid-structure interaction problems is basically considered as three fields i.e. structural deformation, fluid flow and moving mesh [19, 20] as shown in Fig. 1. The governing equation for these types of problems can be written as.
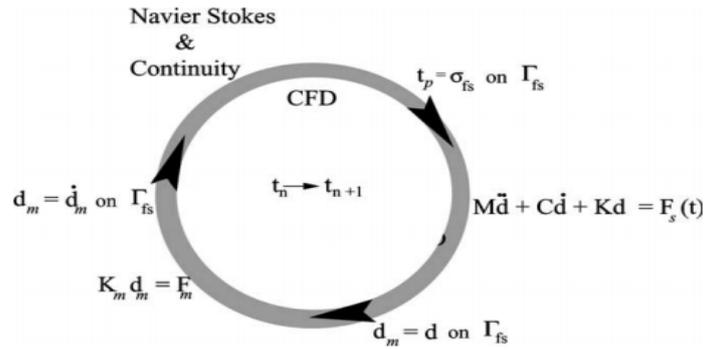
Figure 1: dynamic fluid structure interaction analysis systems[21]

For compressible flow general form of Navier-stokes equation is given below.

$$\frac{\partial}{\partial t}(\rho u_i) + \nabla.\rho u u_i = -\nabla p + \nabla.\mu \nabla u_i + F_f(t)$$

(1)

And associated continuity equation is

$$\frac{\partial p}{\partial t} + \nabla.\rho u = 0$$

(2)

In case of dynamic mesh the velocity relative to the mesh movement can be written as:

$$u = u_{fluid} - u_{mesh} \cdot$$

Dynamic response of structural is governed by following equation which is written as following in matrix form

$$M\ddot{d} + C\dot{d} + Kd = F_s(t)$$

(3)

Whereas

$$F_s = F^{ext} + F^{int}$$

Here damping constant of structure is approximated by Rayleigh damping, where damping matrix C would be formed by linear combination of mass and stiffness matrix.

$$C = \alpha_r M + \beta_r M$$

(4)

Mesh movement may be modeled as a pseudo-structural problem with its own dynamics, with

66

a spring based mesh [22] then the governing equation will be:

$$K_m d_m = f_m(t)$$ (5)

In the absence of any other boundary conditions, the method for integrating the flow equations should preserve the solution of the NS and continuity equations. This condition is Satisfied only when the method for solving the flow equations and the algorithm for updating the displacement and velocity of the mesh obey the geometric conservation law [20, 23].

3. Dynamic mesh movement governing equation

Dynamic mesh is used for those flows where domain shape is continuously changing with the time on the boundaries of domain. The volume mesh updates are automatically handled by FLUENT at each time steps according to new boundary positions. In those cases mesh movement is governed by static displacement Eq. (6)

$$K_m \xi(t) = f\left(d\left(t\right)\right)$$ (6)

4. Aircraft wing Modeling

In this research rectangular aircraft wing is designed because it is widely used in propeller aircraft. Wing is designed with airfoil NACA2412 whose co-ordinates are taken from National Advisory Space Administration (NASA) website.

Wing is designed with chord and span of 200mm and 600 mm respectively. Three dimensional model of wing is imported to ANSYS software where the fluid domain around the wing is generated in ANSYS design modeler to simulate flow effects. Solid aircraft wing is then subtracted from fluid domain by preserving both fluid as well as structural domain

4.1 CSD and CFD models

In case of CSD only structural part is dealt, in this case that is simplified model of aircraft wing without flaps and it was considered as solid wing. Aircraft wing was meshed by using beam elements of tetrahedral shape. Non- conforming mesh algorithm was applied to generated staggered mesh so that high pressure gradient regions were mesh with highly fine elements.

The one end of wing was clamped as it is fixed aircraft body, so wing behavior was studied by assuming it as cantilever beam. Wing was modeled and simulated by using Aluminum alloy 7075-T6 that is widely used in various aircraft parts.

The Mechanical properties of Aluminum alloy 7075-T6 are given below. Fig. 5 presents wing model with applied loads and constrains.

Table1: Showing mesh information of fluid domain

Domain	Element type	orthogonal quality	Nodes	Elements
Fluid	Tetrahedral	0.86	162497	920248

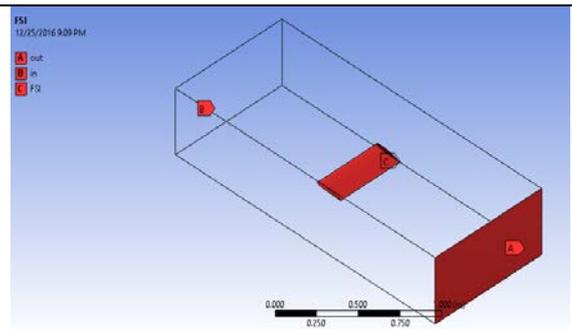**Table 2:** Mechanical properties of Aluminum alloy 7075-T6 [27].

Density Kg/m^3	Modulus of elasticity(GPa)	Shear Strength (MPa)	Ultimate Tensile Strength (MPa)	Tensile Strength, Yield (MPa)	Creep Strength(MPa)	Rupture Strength (MPa)
2810	71.7	317	524	462	515	530

Table 3: Showing mesh information of solid domain

| Domain	Element type	Orthogonal quality	Nodes	Elements
Solid Wing	Tetrahedral	0.80	5303	1924
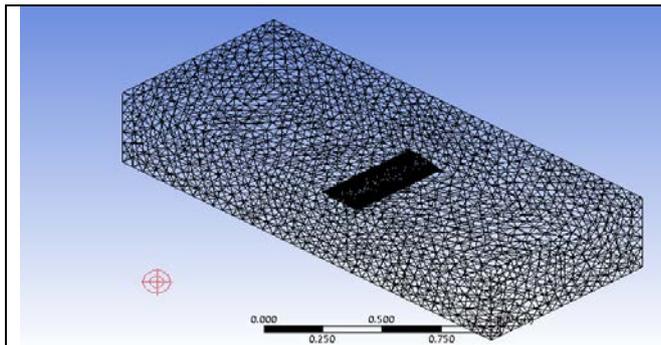
Figure 2: Mesh of fluid domain	**Figure 3:** Named sections of fluid domain

In case of CFD model simplified model of aircraft wing surrounded by fluid domain were modeled. Meshing of turbine was carried out in ANSYS ICEM where tetrahedral mesh elements were used to generate control volumes. Non-uniform unstructured mesh was generated through applying non-conforming algorithm to

improve mesh quality in the region of high pressure gradients. Names to various boundaries of model were assigned in order to apply boundary conditions during simulation. Meshed model of wing in CFD model is presented in 2.
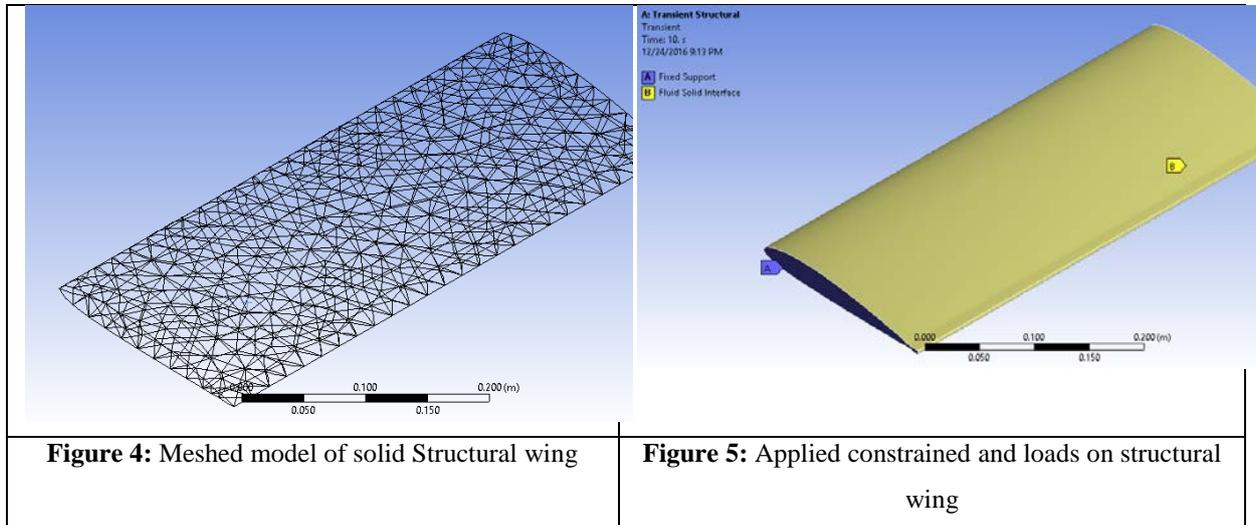
| **Figure 4:** Meshed model of solid Structural wing | **Figure 5:** Applied constrained and loads on structural wing |

5. Computational Methodology

In order to solve two-way-FSI problem solver of computational fluid Dynamics and computational solid dynamics are coupled. Loosely coupled partitioned approach was used to exchange the data between to solvers. Wing FSI analysis was carried out at free stream condition of M=0.4 and angle of attack α =5° because that is maximum speed at which propeller aircraft fly. In two way FSI analysis both the CFD and CSD solvers are running simultaneously, to transfer instantaneous data. In CSD three sides of wing receives fluid forces and deformation caused by those aerodynamic forces would be transferred to CFD model in order to evaluate effect of wing deformation. In CFD turbulences were modeled through k-ω SST model and compressibility effects was encountered by selecting density based model. This study uses SST k-ω model is more suitable for near wall treatment to analyze boundary layer and flow separation problems [24-26]. Dynamic meshing is done and in which wing is allowed to deflect in correspondence of fluid forces. System coupling region is created to receive updated mesh from structural solver. Implicit scheme, pressure velocity coupling and second order discretization scheme is used to solve time dependent fluid domain. After completion of individual setup system coupling was updated to solve FSI problem through getting data from CFD and CSD solvers

6. Results and Discussion

In this section results of dynamic fluid structure interaction are presented separately for both structural and fluid flow parts.

6.1 Structural analysis

Dynamic fluid structure interaction analysis is conducted in order to simulate and analyze effect of real flight. To carry out structural analysis fluid forces are transferred to structural module. Stresses and deformation occurs in aircraft wing was determined corresponding to those fluid forces. Simulation results are presented in table below for the time period of 4 seconds. By analyzing the variation in stresses and deformation it is clear that they are highly time-dependent in nature. Through careful analysis of Von-Mises stresses, maximum shear stresses and deformation during first four time steps they have achieved highest value of 165MPa, 90.8MPa and 14.1mm respectively.

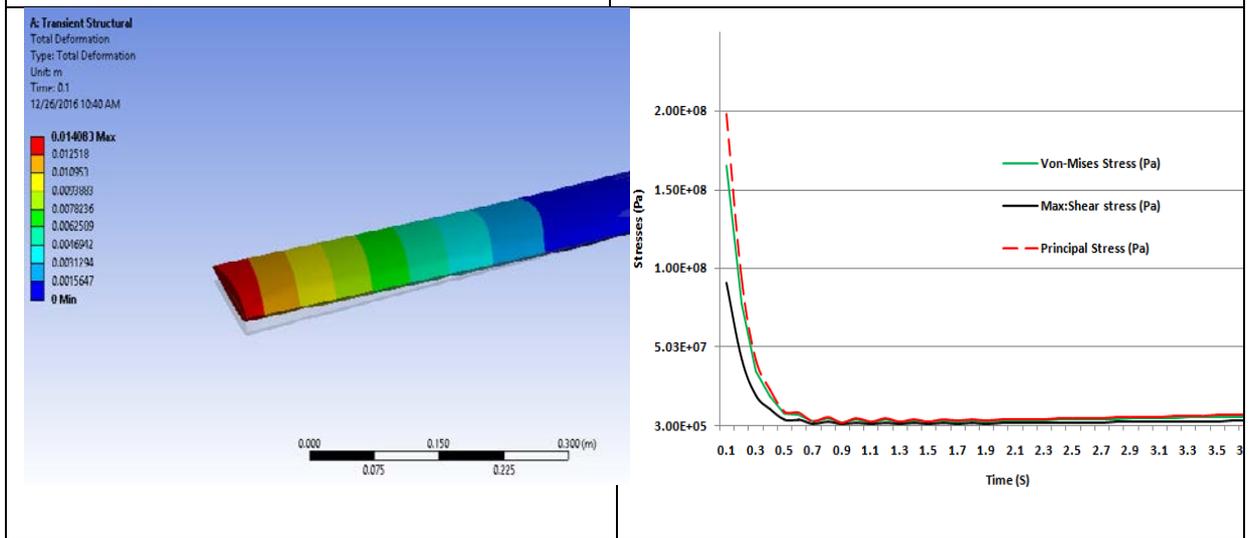**Table 4:** Shows the variation of stresses and deformation with flight time

Simulation Time(s)	Von-Mises stress (Pa)	Max. Shear stress (Pa)	Max: Principal stress (Pa)	Total Deformation(m)
0.1	1.65E+08	9.08E+07	1.98E+08	1.41E-02
0.2	7.79E+07	4.29E+07	9.36E+07	6.67E-03
0.3	3.49E+07	1.92E+07	4.20E+07	2.97E-03
0.4	1.91E+07	1.05E+07	2.29E+07	1.63E-03
0.5	7.71E+06	4.25E+06	9.30E+06	6.33E-04
0.6	7.20E+06	3.97E+06	8.56E+06	6.05E-04
0.7	2.55E+06	1.41E+06	3.12E+06	1.91E-04
0.8	4.88E+06	2.69E+06	5.84E+06	4.06E-04
0.9	1.94E+06	1.07E+06	2.41E+06	1.41E-04
1	4.27E+06	2.35E+06	5.13E+06	3.52E-04
1.1	2.06E+06	1.14E+06	2.55E+06	1.55E-04
1.2	3.92E+06	2.16E+06	4.73E+06	3.22E-04
1.3	2.29E+06	1.26E+06	2.82E+06	1.77E-04
1.4	3.68E+06	2.03E+06	4.45E+06	3.02E-04
1.5	2.51E+06	1.39E+06	3.09E+06	2.00E-04
1.6	3.49E+06	1.93E+06	4.24E+06	2.87E-04
1.7	2.69E+06	1.49E+06	3.31E+06	2.16E-04
1.8	3.40E+06	1.87E+06	4.13E+06	2.78E-04
1.9	2.92E+06	1.61E+06	3.58E+06	2.34E-04
2	3.46E+06	1.91E+06	4.22E+06	2.81E-04
2.1	3.23E+06	1.78E+06	3.95E+06	2.58E-04
2.2	3.67E+06	2.02E+06	4.47E+06	2.94E-04
2.3	3.61E+06	1.99E+06	4.41E+06	2.86E-04
2.4	3.96E+06	2.18E+06	4.82E+06	3.14E-04
2.5	4.01E+06	2.21E+06	4.89E+06	3.16E-04
2.6	4.29E+06	2.37E+06	5.22E+06	3.38E-04
2.7	4.37E+06	2.41E+06	5.32E+06	3.43E-04
2.8	4.57E+06	2.52E+06	5.56E+06	3.60E-04
2.9	4.68E+06	2.58E+06	5.68E+06	3.68E-04
3	4.85E+06	2.68E+06	5.89E+06	3.82E-04
3.1	5.00E+06	2.76E+06	6.06E+06	3.94E-04
3.2	5.19E+06	2.86E+06	6.28E+06	4.10E-04
3.3	5.35E+06	2.95E+06	6.47E+06	4.24E-04
3.4	5.51E+06	3.04E+06	6.66E+06	4.37E-04
3.5	5.63E+06	3.10E+06	6.80E+06	4.47E-04
3.6	5.74E+06	3.16E+06	6.93E+06	4.55E-04
3.7	5.85E+06	3.22E+06	7.07E+06	4.64E-04
3.8	5.96E+06	3.29E+06	7.20E+06	4.73E-04
3.9	6.09E+06	3.36E+06	7.36E+06	4.83E-04
4	6.21E+06	3.43E+06	7.50E+06	4.93E-04

The following Fig.7, 8 and 9 show the variation of principal stress, max: shear stresses and deformation occurs in aircraft wing. In all of these Figures both deformed and un-deformed model of wing are shown, which is highly helpful in visualizing the wing deformation due to fluid pressure. In Fig. 8 the maximum and minimum shear stress points are highlighted which shown that maximum stresses occurs near the fixed edge of wing. In Fig.9 the wing deformation is shown throughout the wing and it can be observed that wing deformation is maximum at wing tip which has value of near about 14.1mm.
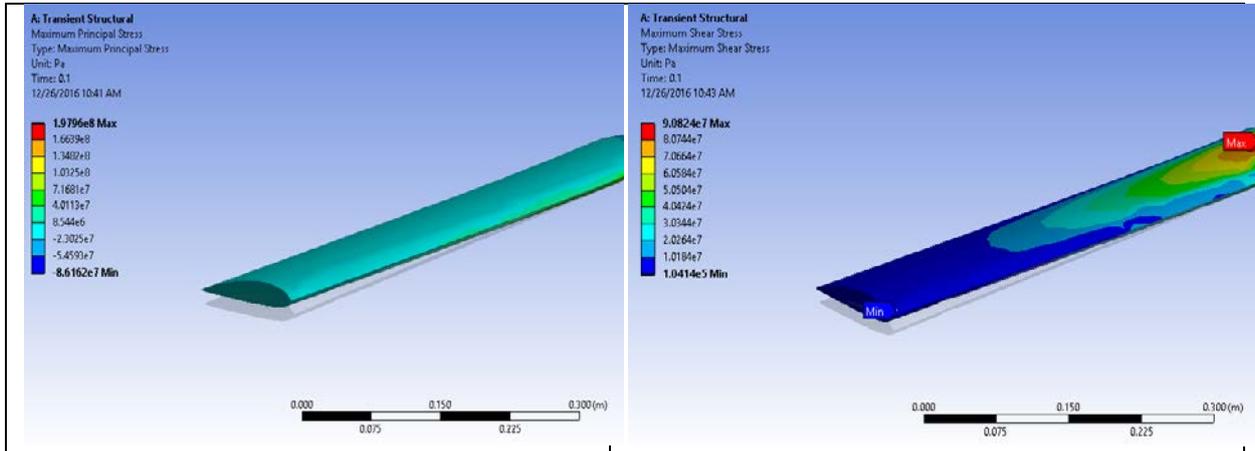
Figure 7: Maximum Principal Stresses in wing	**Figure 8:** Maximum Shear Stresses in wing
Figure 9: Showing aircraft wing deformation	**Figure 10:** Shows variation of stresses and deformation with time

6.2 Fluid flow analysis

In this second part of results and discussion, the results of fluid flow are presented. In dynamic fluid structure interaction time-dependent initial conditions are applied and realistic results were obtained through computer simulation. In dynamic FSI problems time varying meshing is introduced in fluent through updating mesh displacement and velocity to analyze effect of deformation on different flow properties. In turns effect of those flow properties influences the overall performance of system. From Fig. 11 & 12 through critically analysis and comparison of flow behavior around the wing is affected by wing deformation. Wing deformation can be clears

observed in highlighted ellipse shown near the wing edge.

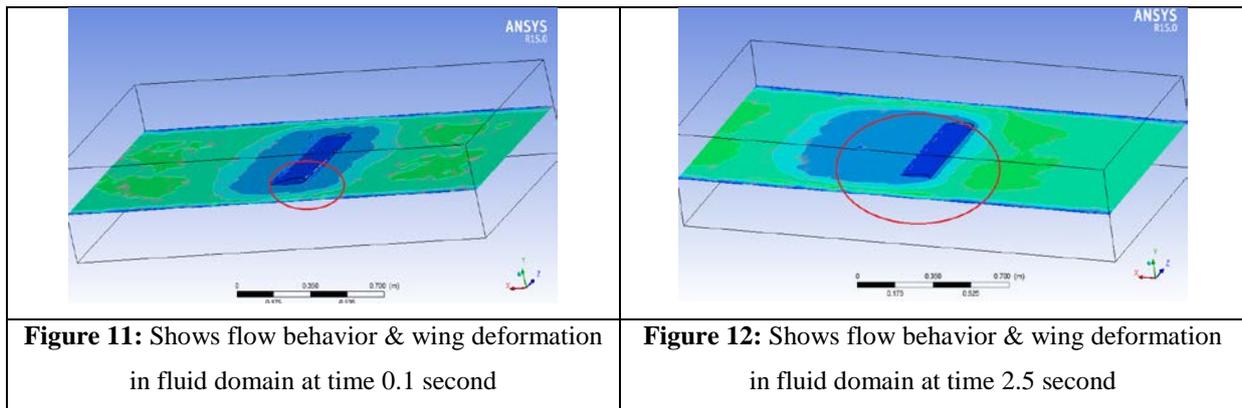|	
Figure 11: Shows flow behavior & wing deformation in fluid domain at time 0.1 second	**Figure 12:** Shows flow behavior & wing deformation in fluid domain at time 2.5 second

Fig. 11 is showing the flow behavior and wing deformation just after 0.1 second. From the structural results of deformation for whole time duration, the deformation and stresses are maximum just after simulation starts, because at the starting energy added by fluid to structure is much higher than that could be handled by structural damping. After some time structural damping would be sufficient to handle flow energy, hence structural deformation decreases with time. Fig. 13 shows the variation of fluid pressure near the deforming wing.
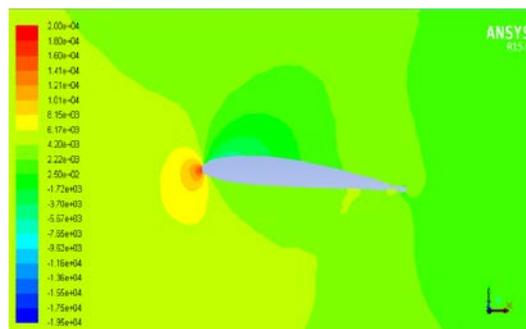
Figure 13: Shows the Pressure variation near the deforming wing.

The dynamic fluid structure interaction and CFD analysis of deformable and rigid was carried out repectivitly to analyze effect of wing deformation on aerodynamic forces. The result simulation reveals that given corresponding values of lift and drag was found for respected wing configuration. From results of simulation it is concluled that L/D ratio decrease as wing deform.

Table 5: Shows the variation of lift and drag for rigid and deforming wing

Wing material	Lift Force (N)	Drag Force (N)	Lift/Drag ratio	% Decrease in L/D ratio	Weight of wing (Kg)	Wing deformation (mm)
Rigid	521.7735	39.744	13.128359			0
Aluminium	491.0127	39.512	12.426926	5.644461073	4.654	14.15

7. Conclusion

In this study dynamic fluid structure interaction analysis was carried out by combining Computational Fluid Dynamics (CFD) and Computational Structural Dynamics (CSD) solver to predict effect of fluid forces on wing structural behaviour and of deformation on aerodynamic efficiency. Research results reveal that there is 5.64% decrease in Lift-to-Drag ratio by considering wing as flexible structure. From the structural results of deformation for whole time duration, the deformation and stresses are maximum just after simulation starts, because at the starting energy added by fluid to structure is much higher than that could be handled by structural damping. After some time structural damping would be sufficient to handle flow energy, hence structural deformation decreases with time. Through analyzing structural behaviour of the wing due to varying fluid forces it is concluded that wing behaviour is highly non-linear in nature, therefore dynamic loading conditions are highly important to consider.

References

[1]. Billah, K. and R. Scanlan, Resonance, Tacoma Narrows bridge failure, and undergraduate physics textbooks. American Journal of Physics, 1991. 59(2): p. 118-24.

[2]. Dooms, D., Fluid-structure interaction applied to flexible silo constructions,, in Department of Civil Engineering. 2008, Katholieke Universiteit Leuven.

[3]. Farhat, C., et al., Provably second-order time-accurate loosely-coupled solution algorithms for transient nonlinear computational aeroelasticity. Computer methods in applied mechanics and engineering 2006. 195(17): p. 1973-2001.

[4]. Willcox, K.E., Reduced-order aerodynamic models for aeroelastic control of turbomachines. 1999, Citeseer.

[5]. Jain, A., N.P. Jones, and R.H. Scanlan, Coupled flutter and buffeting analysis of long-span bridges. Journal of Structural Engineering, 1996. 122(7): p. 716-725.

[6]. Yang, J.N., et al., Benchmark problem for response control of wind-excited tall buildings. Journal of Engineering Mechanics, 2004. 130(4): p. 437-446.

[7]. Arrigan, J., et al., Control of flapwise vibrations in wind turbine blades using semi-active tuned mass dampers. Structural Control and Health Monitoring, 2011. 18(8): p. 840-851.

[8]. De Langre, E., Effects of wind on plants. Annu. Rev. Fluid Mech., 2008. 40: p. 141-168.

[9]. Wan, Z. and C. Yang, Aeroelastic optimization of a high-aspect-ratio composite wing. Fuhe Cailiao Xuebao(Acta Mater. Compos. Sin.), 2005. 22(3): p. 145-149.

[10]. SI, L., H.-p. Wang, and C.-c. Gong, Investigation of Effects of Winglets on Wing′s Flutter Behavior [J]. Aeronautical Computing Technique, 2009. 4: p. 023.

[11]. Changchuan, X., W. Zhigang, and Y. Chao, Aeroelastic analysis of flexible large aspect ratio wing. JOURNAL-BEIJING UNIVERSITY OF AERONAUTICS AND ASTRONAUTICS, 2003. 29(12; ISSU 130): p. 1087-1090.

[12]. Tielin, Z.H.M.D.M., Analysis of aerodynamics characteristic of flexible wing caused by deflection [J]. Journal of Beijing University of Aeronautics and Astronautics, 2008. 5: p. 002.

[13]. Hua, M.T.M.D.Z., Aerodynamic characteristic analysis of high-aspect ratio elastic wing [J]. Journal of

Beijing University of Aeronautics and Astronautics, 2007. 7: p. 009.

[14]. Shi, A.-M., Y.-N. Yang, and G. Wang, Investigations of characteristics of static aeroelasticity for elastic wing in transonic flow [J]. Engineering Mechanics, 2006. 23(5): p. 173-176.

[15]. Liu, G.-c. and Z.-h. Xie, Design and Analysis of High Aspect Ratio Composite Wing [J]. Aircraft Design, 2008. 6: p. 005.

[16]. Huo, S.-h., et al., Effects of static aeroelasticity on composite wing characteristics under different flight attitudes. Journal of Central South University, 2013. 20: p. 312-317.

[17]. Smith, M.J., D.H. Hodges, and C.E. S. Cesnik, Evaluation of computational algorithms suitable for fluid-structure interactions. Journal of Aircraft, 2000. 37(2): p. 282-294.

[18]. Zhu, J., et al., Numerical study of a variable camber plunge airfoil under wind gust condition. Journal of Mechanical Science and Technology, 2015. 29(11): p. 4681-4690.

[19]. Farhat, C., M. Lesoinne, and N. Maman, Mixed explicit/implicit time integration of coupled aeroelastic problems: Three-field formulation, geometric conservation and distributed solution. International Journal for Numerical Methods in Fluids, 1995. 21(10): p. 807-835.

[20]. Thomas, P. and C. Lombard, Geometric conservation law and its application to flow computations on moving grids. AIAA journal, 1979. 17(10): p. 1030-1037.

[21]. Slone, A., et al., A finite volume unstructured mesh approach to dynamic fluid–structure interaction: an assessment of the challenge of predicting the onset of flutter. Applied mathematical modelling, 2004. 28(2): p. 211-239.

[22]. Batina, J.T., Unsteady Euler airfoil solutions using unstructured dynamic meshes. AIAA journal, 1990. 28(8): p. 1381-1388.

[23]. Lesoinne, M. and C. Farhat, Geometric conservation laws for aeroelastic computations using unstructured dynamic meshes. AIAA paper, 1995(95-1709).

[24]. Menter, F. and Y. Egorov, The scale-adaptive simulation method for unsteady turbulent flow predictions. Part 1: theory and model description. Flow, Turbulence and Combustion, 2010. 85(1): p. 113-138.

[25]. Menter, F.R., Performance of popular turbulence model for attached and separated adverse pressure gradient flows. AIAA journal, 1992. 30(8): p. 2066-2072.

[26]. Mylavarapu, G., et al., Validation of computational fluid dynamics methodology used for human upper airway flow simulations. Journal of biomechanics, 2009. 42(10): p. 1553-1559.

[27]. http://www.matweb.com/